Linear stability analysis of walking vector solitons

Dumitru Mihalache, Dumitru Mazilu, and Lucian-Cornel Crasovan
Department of Theoretical Physics, National Institute of Physics and Nuclear Engineering, Institute of Atomic Physics, P.O. Box MG-6, Bucharest, Romania

(Received 25 March 1999; revised manuscript received 23 July 1999)

The linear stability analysis of two-parameter families of walking vector solitons of coupled nonlinear Schrödinger equations is performed. It is shown that the eigenvalues of the corresponding linearized problem can be complex valued in certain regions of the parameter space. The complex nature of the associated Lyapunov eigenvalues leads to a quite complicated pattern of instability regions of lowest-order soliton types. This pattern includes two typical situations: (i) the relevant eigenmode has a purely imaginary eigenvalue that passes through zero at the critical point and then becomes purely real, and (ii) the interplay between two discrete eigenmodes having purely imaginary eigenvalues leads to a bifurcation scenario where two imaginary eigenvalues merge together and become complex at the bifurcation point. It is shown that all known, lowest-order soliton types, namely slow, fast, in-phase vector, and out-of-phase vector, are dynamically stable in certain regions of the parameter space. [S1063-651X(99)00912-5]

PACS number(s): 42.65.Tg, 42.81.Dp, 41.20.Jb

I. INTRODUCTION

Solitons are ubiquitous entities which can be thought of as the nonlinear eigenmodes of certain dynamical systems [1]. They play a fundamental role in many branches of nonlinear science, from both a theoretical and applied point of view. The balance between linear dispersing (or diffracting) effects and nonlinear effects gives rise to the formation of these objects which are remarkably robust against various perturbations of the considered physical system. The solitons are thus stable solutions of completely integrable evolution equations, but this is not necessarily so for the solitary waves arising in physical systems modeled by nonintegrable nonlinear evolution equations [2]. Understanding the stability of solitary waves is a key issue of nonlinear physics because of its direct connection with the possibility of experimental observation of these rather robust objects. Important applications of solitons, or, more properly, solitary waves in optical transmission systems and devices are just emerging and the study of optical solitary waves in a variety of physical settings generates a continuously renewed interest [3,4].

When weak nonlinearity and dispersion are present in the considered physical system, the envelopes of quasimonochromatic waves obey the nonlinear Schrödinger equation (NLSE) and its vector versions, that is, a system of two (or more) coupled NLSEs. In this case one can naturally expect that the mode interaction gives rise to many-component (vector) solitons, and therefore the elucidation of the dynamical stability of such entities is of paramount importance.

The stability of many one-parameter families of bright solitary-wave solutions of Hamiltonian, nonintegrable dynamical systems is well established [5–7], and stability criteria based on the conserved quantities of the evolution that hold for several soliton families are known. A typical example is the so-called Vakhitov-Kolokolov criterion [5], which is known to hold for several one-parameter soliton families, including generalized NLSEs and the equations describing some quadratic solitons. The stability of one-parameter families of soliton solutions of various kinds of generalized Manakov equations describing propagation of temporal vector optical solitons has been studied in a number of works [8]. However, the stability features of multiple-parameter soliton families is much richer than commonly believed, and by and large constitutes a challenging problem. Examples, very important from the physical point of view, and closely related to the dynamical system examined in the present paper, include two-parameter families of three-wave quadratic solitons [9], two-wave and three-wave walking quadratic solitons [10], walking vector solitons of coupled NLSEs [11–13], gap solitons existing in periodic structures with cubic or quadratic nonlinearities [14–16], or solitons of generalized massive Thirring models in the presence of dispersion [17].

New instability mechanisms of higher-order modes in planar waveguides containing cubic nonlinear media [18] and of higher-order peak-and-ring solitons in quadratic nonlinear media [19] linked to the non-Hermitian nature of the linearized perturbed evolution operator were discovered. Oscillatory instabilities for ground-state (nodeless) gap solitons existing in cubic nonlinear media due to the non-self-adjointess of the Lyapunov operator were found recently [20].

In this paper, we investigate in detail the instability scenarios of the existing families of bright, lowest-order walking vector solitons of general coupled NLSEs [21]. The model considered is a generalized Manakov system [22–25] originally derived by Menyuk [26] to describe pulse propagation in birefringent optical fibers in the presence of walk-off, self-phase modulation, cross-phase modulation, and three-wave mixing between the linearly polarized modes of the fiber. Such a system offers the additional motivation of the important applications of the phenomena uncovered to ultrafast devices for information processing [27–29].

The organization of this paper is as follows. In Sec. II, a thorough numerical analysis of the linear stability of the stationary solutions of the general coupled NLSEs is performed, the relevant instability scenarios are identified, and a mechanism for the onset of the oscillatory instability is put into evidence. The main results of this paper are summarized in the final section.

 © 1999 The American Physical Society

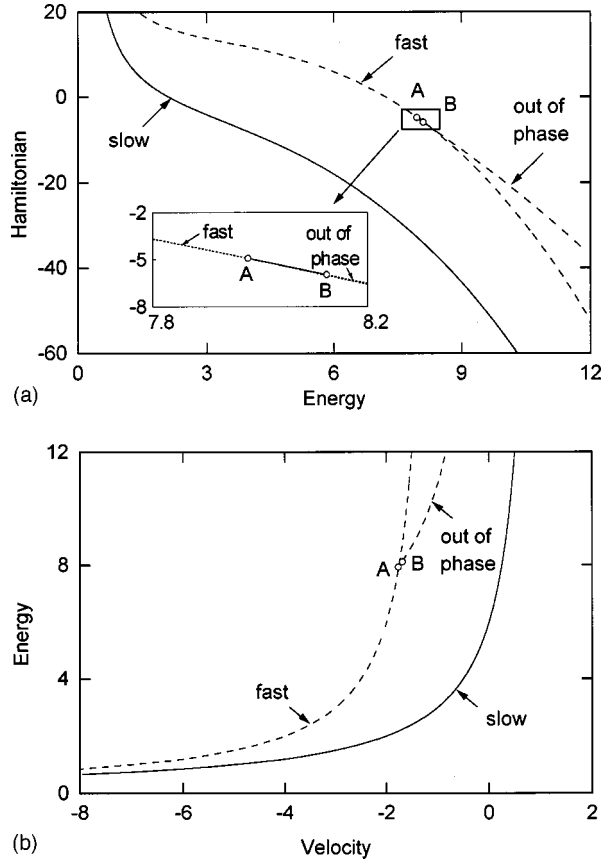

FIG. 1. (a) Hamiltonian versus energy, and (b) energy versus velocity for the families of walking vector solitons at fixed momentum $M=-6$. Full lines: stable solitons. Dashed lines: unstable solitons. The meaning of the marked points is explained in the text.

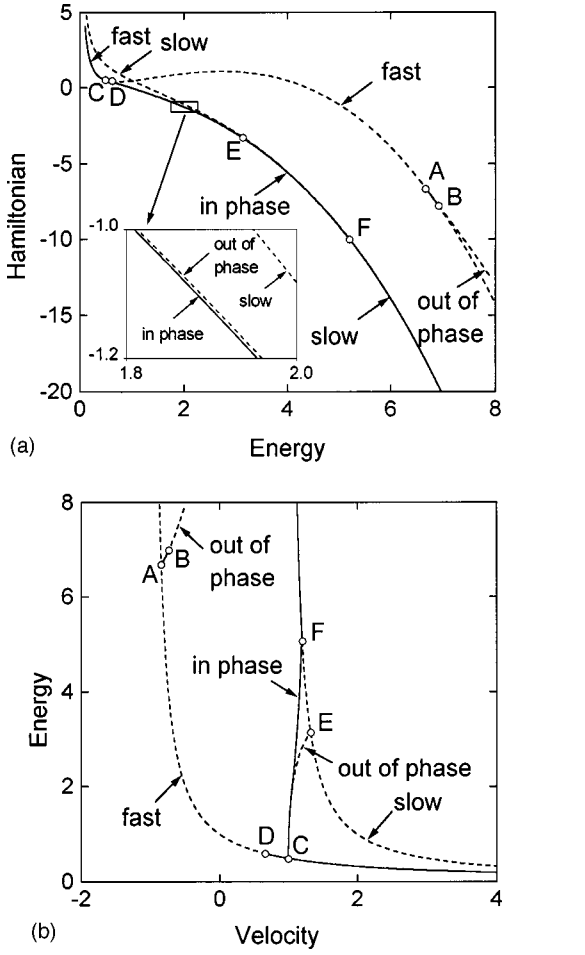

FIG. 2. Same as in Fig. 1 but for $M=1$.

II. LINEAR STABILITY ANALYSIS

We consider solitary-wave formation in a dynamical system described by the vector NLSE in the generic form [26]

$$i\frac{\partial U}{\partial \xi}+\beta U+i\delta\frac{\partial U}{\partial s}+\frac{1}{2}\frac{\partial^2 U}{\partial s^2}+(|U|^2+A|V|^2)U+BV^2U^*=0, \tag{1}$$

$$i\frac{\partial V}{\partial \xi}-\beta V-i\delta\frac{\partial V}{\partial s}+\frac{1}{2}\frac{\partial^2 V}{\partial s^2}+(|V|^2+A|U|^2)V+BU^2V^*=0.$$

In the case of pulse propagation in a birefringent fiber, U and V are the amplitudes in each polarization, ξ is the normalized propagation coordinate, s is the normalized time coordinate, δ is proportional to the group velocity difference between the two polarizations, β is half the difference between the propagation wave numbers, the constant A depends on the modal properties of the optical fiber, and $B=1-A$. In linearly birefringent fibers, $A=2/3$, as we set here. We consider here the regime where the walk-off length associated to δ, and the birefringence beat length associated to β, are comparable to the nonlinear scale length. In all the numerical calculations presented in this paper, we set the parameters $\beta=1$ and $\delta=1$. Notice that the dynamical system (1) possesses only three conserved quantities of the pulse evolution, namely the energy

$$Q=\int (|U|^2+|V|^2)ds, \tag{2}$$

the momentum

$$M=\frac{1}{2i}\int\left[\left(U^*\frac{\partial U}{\partial s}-U\frac{\partial U^*}{\partial s}\right)+\left(V^*\frac{\partial V}{\partial s}-V\frac{\partial V^*}{\partial s}\right)\right]ds, \tag{3}$$

and the Hamiltonian

$$H=\frac{1}{2}\int\left\{\left(\left|\frac{\partial U}{\partial s}\right|^2+\left|\frac{\partial V}{\partial s}\right|^2\right)-[|U|^4+|V|^4]-2\beta[|U|^2-|V|^2]-2A|U|^2|V|^2-(1-A)[U^2V^{*2}+U^{*2}V^2]-i\delta\left(U^*\frac{\partial U}{\partial s}-U\frac{\partial U}{\partial s}^*-V^*\frac{\partial V}{\partial s}+V\frac{\partial V}{\partial s}^*\right)\right\}ds. \tag{4}$$

The stability of soliton solutions of truncated versions of Eqs. (1), without the terms with the coefficients δ or B, has been studied in a number of works [8]. However, the existence of different kinds of two-parameter families of walking vector (in-phase and out-of-phase) and scalar (slow and fast) solitons arising in the physical system modeled by the untruncated Hamiltonian dynamical system (1) was first investigated in Ref. [11]. Moreover, it was found there that, when the group-velocity difference is high enough, both slow and fast linearly polarized solitons are unstable. A comprehen-

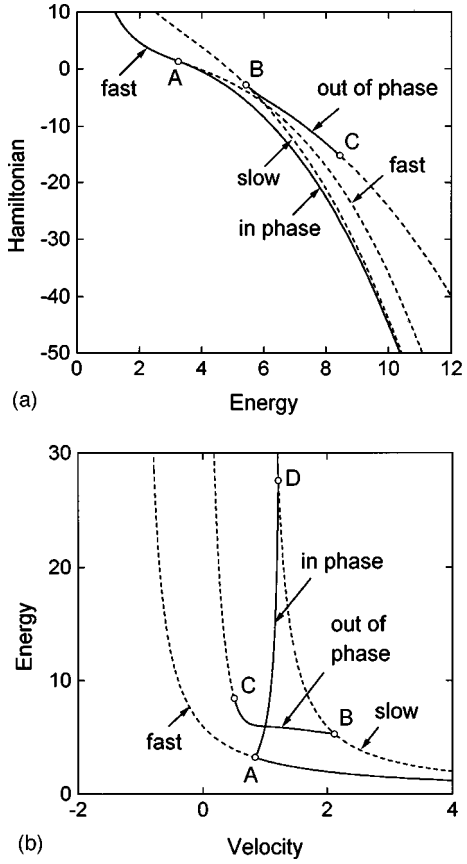

FIG. 3. Same as in Fig. 1 but for $M=6$.

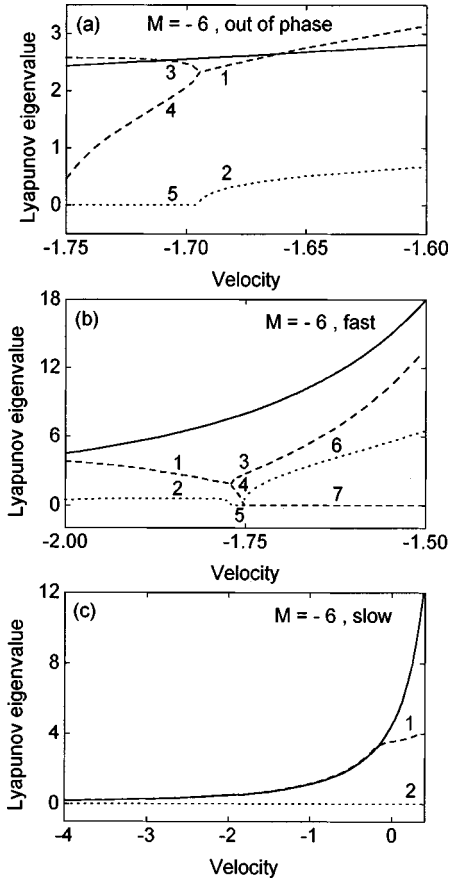

FIG. 4. The eigenvalue versus velocity for $M=-6$. Dotted lines: real part. Dashed lines: imaginary part. The full lines show the lower bound of the continuous spectrum. (a) Out-of-phase soliton branching out from the fast one, (b) fast, and (c) slow.

sive study of the characteristic features of the two-parameter family of walking vector solitons of the generalized Manakov model was performed in Ref. [13]. The aim of the present paper is to expand on the work [21], in order to identify the mechanism responsible for the onset of oscillatory instabilities, and to get the corresponding regions of oscillatory instabilities in the space of the soliton parameters.

First of all, by using a multiscale asymptotic method [9], we derive the condition of marginal stability of the two-parameter family of walking vector solitons. We first make the change of coordinates $\tau=s-v\xi$ and $\zeta=\xi$ in Eqs. (1) and we look for solutions of the form $U=u(\tau,\zeta)e^{iq\zeta}$ and $V=v(\tau,\zeta)e^{iq\zeta}$. Let $\mathbf{c}_0=\mathbf{c}_0(\tau)=(u_r^s,v_r^s,u_i^s,v_i^s)^T$ be the column vector formed with the stationary walking vector solitons $u_s=u_r^s+iu_i^s$, $v_s=v_r^s+iv_i^s$. To analyze the stability of these solutions with respect to small perturbations, we substitute $\mathbf{c}(\tau,\zeta)=\mathbf{c}_0(\tau)+\varepsilon\mathbf{c}_1(\tau)e^{\lambda\zeta}$, where $\mathbf{c}_1=(u_{1r},v_{1r},u_{1i},v_{1i})^T$ and ε is a small parameter, into Eqs. (1) and linearize the resulting equations obtaining a linear eigenvalue problem $\mathbf{A}\mathbf{c}_1=\lambda\mathbf{g}$, where $\mathbf{A}$ is a self-adjoint operator and $\mathbf{g}=(u_{1i},v_{1i},-u_{1r},-v_{1r})^T$. For $\lambda=0$, this eigenvalue problem has two spatially localized solutions,

$$\frac{\partial\mathbf{c}_0}{\partial\tau},\quad (u_i^s,v_i^s,-u_r^s,-v_r^s)^T, \tag{5}$$

giving the neutrally stable modes. In order to find a threshold condition for the linear instability, we consider that the instability growth rate λ is small, so that we can seek solutions of the above linear eigenvalue problem in the form of asymptotic series in the small parameter λ: $\mathbf{c}_1=\Sigma_{j=0}^{\infty}\lambda^j\mathbf{c}_1^{(j)}$, where $\mathbf{c}_1^{(j)}=(u_r^{(j)},v_r^{(j)},u_i^{(j)},v_i^{(j)})^T$. We introduce also the series $\mathbf{g}=\Sigma_{j=0}^{\infty}\lambda^j\mathbf{g}^{(j)}$, where $\mathbf{g}^{(j)}=(u_i^{(j)},v_i^{(j)},-u_r^{(j)},-v_r^{(j)})^T$. Substituting the above expansions into the linearized equations and collecting terms of the same order in λ, we find the following explicit analytical solutions for the first-order corrections $-\partial\mathbf{c}_0/\partial v$ and $-\partial\mathbf{c}_0/\partial q$. The instability threshold condition emerges at the next, second order in λ. Thus, in the second order we get $\mathbf{A}\mathbf{c}_1^{(2)}=\mathbf{g}^{(1)}$. Next we use the following property of a self-adjoint operator $\mathbf{A}$: let $\mathbf{a}_0$ belong to the kernel space of the operator $\mathbf{A}$ ($\mathbf{A}\mathbf{a}_0=0$) and let $\mathbf{b}$ belong to the image space of the operator $\mathbf{A}$ ($\mathbf{A}\mathbf{a}=\mathbf{b}$); then the vectors $\mathbf{a}_0$ and $\mathbf{b}$ are orthogonal to each other. By imposing this orthogonality relation, we are left with a linear homogeneous system of equations and its solvability condition gives the equation defining the curve of marginal stability: $J=\partial(Q,M)/\partial(q,v)=0$. This condition (but a sufficient one) corresponds to the loci where the surface (Q,M,H) exhibits a *folding* and can also be derived using pure geometrical approaches [7].

By calculating the Jacobian for the families of walking vector solitons, one finds that $J=4$ for all the slow and fast solitons. In the case of vector in-phase and of vector out-of-phase solitons, the value of J depends on the soliton considered. However, for all the vector soliton families that we examined numerically, the important result found is that J

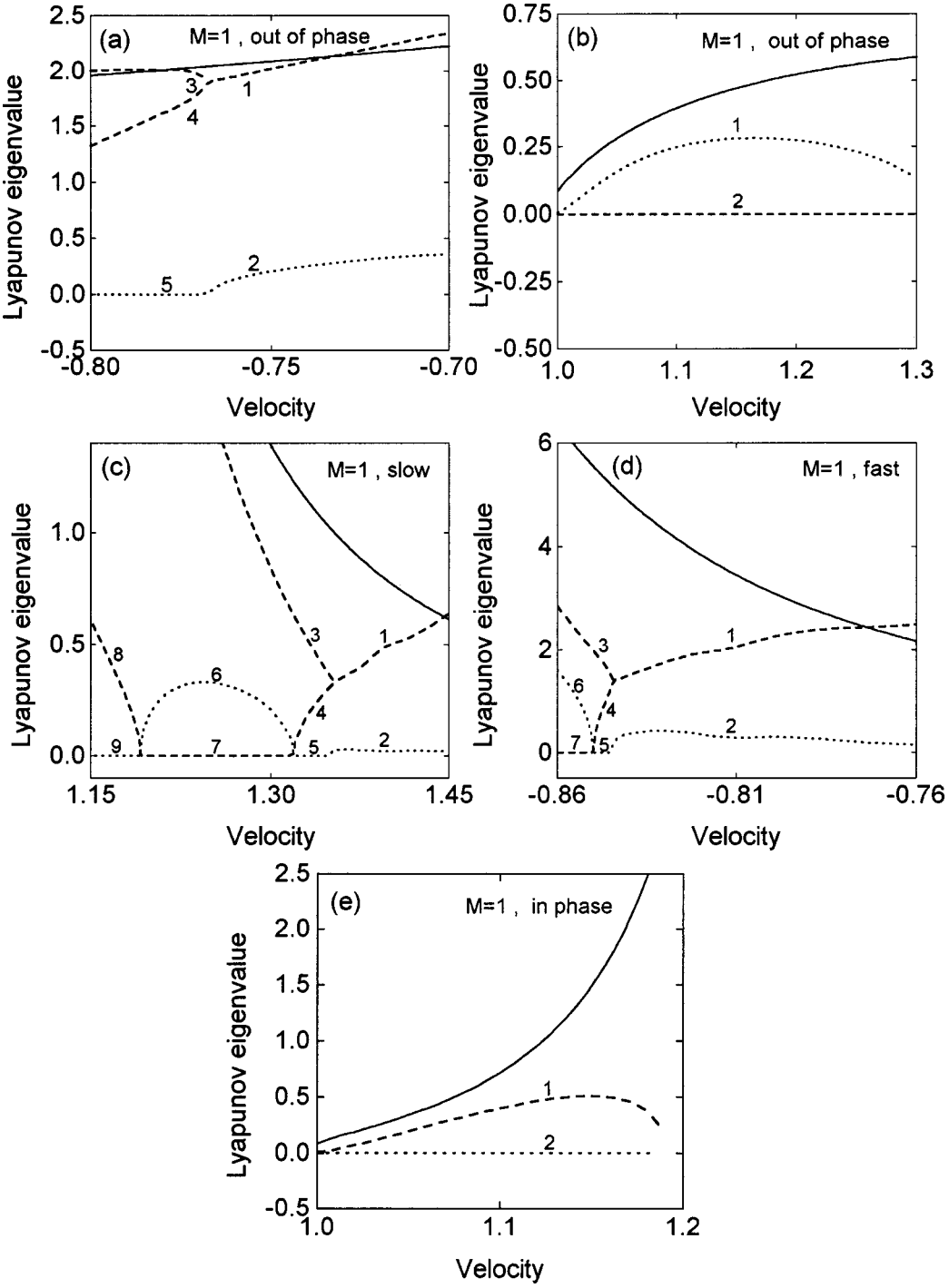

FIG. 5. Same as in Fig. 4 but for $M=1$. (a) Out-of-phase soliton branching out from the fast one, (b) out-of-phase soliton branching out from the slow one, (c) slow, (d) fast, and (e) in-phase.

never vanishes. Yet, the existence of unstable walking vector soliton solutions is readily exposed by solving Eqs. (1) numerically and considering different stationary solutions as input conditions. As a typical example, we found that the unstable vector out-of-phase soliton reshapes into a stable vector in-phase soliton. This process is accompanied by a change of the velocity of the input soliton [21]. Therefore, in order to find the stability domains of walking vector solitons, we proceed as follows.

First we linearize the evolution equations (1) around the stationary walking vector soliton and obtain the following eigenvalue problem: $\mathbf{L}\mathbf{c}_1=\lambda\mathbf{c}_1$, where the column vector $\mathbf{c}_1$, defined above, is the small perturbation. The linearized non-self-adjoint operator $\mathbf{L}$ is a 4×4 matrix having the following elements: $l_{11}=-(\delta-v)(\partial/\partial\tau)-2u_r^s u_i^s-2(1-A)v_r^s v_i^s$, $l_{22}=(\delta+v)(\partial/\partial\tau)-2v_r^s v_i^s-2(1-A)u_r^s u_i^s$, $l_{33}=-(\delta-v)(\partial/\partial\tau)+2u_r^s u_i^s+2(1-A)v_r^s v_i^s$, $l_{44}=(\delta+v)(\partial/\partial\tau)+2v_r^s v_i^s+2(1-A)u_r^s u_i^s$, $l_{31}=(\beta-q)+\frac{1}{2}(\partial^2/\partial\tau^2)+3u_r^{s2}+u_i^{s2}+v_r^{s2}+(2A-1)v_i^{s2}$, $l_{42}=-(\beta+q)+\frac{1}{2}(\partial^2/\partial\tau^2)$

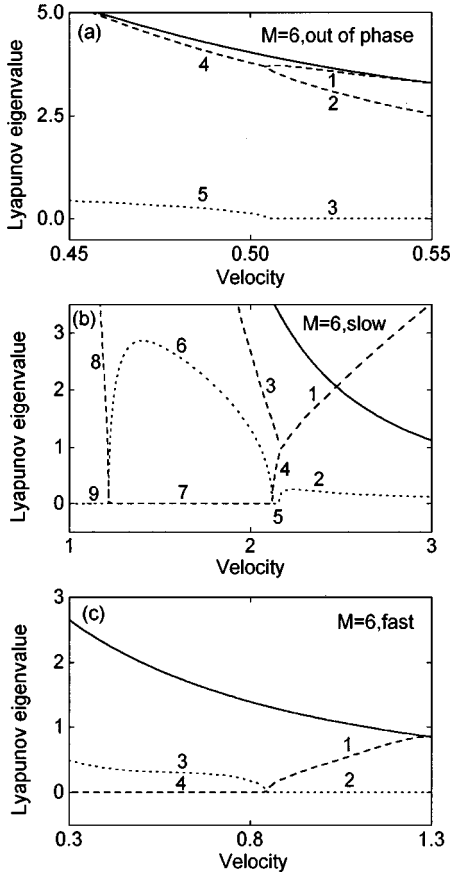

FIG. 6. Same as in Fig. 4 but for $M=6$. (a) Out-of-phase soliton branching from the slow one, (b) slow, and (c) fast.

$+3v_r^{s2}+v_i^{s2}+u_r^{s2}+(2A-1)u_i^{s2}$,
$l_{13}=-(\beta-q)-\frac{1}{2}(\partial^2/\partial\tau^2)-3u_i^{s2}-u_r^{s2}-v_i^{s2}-(2A-1)v_r^{s2}$,
$l_{24}=(\beta+q)-\frac{1}{2}(\partial^2/\partial\tau^2)-3v_i^{s2}-v_r^{s2}-u_i^{s2}-(2A-1)u_r^{s2}$,
$l_{32}=l_{41}=2u_r^s v_r^s+2(1-A)u_i^s v_i^s$, $l_{34}=-l_{21}=2(2A-1)u_r^s v_i^s+2(1-A)u_i^s v_r^s$, $l_{43}=-l_{12}=2(2A-1)u_i^s v_r^s+2(1-A)u_r^s v_i^s$, $l_{14}=l_{23}=-2u_i^s v_i^s-2(1-A)u_r^s v_r^s$.

Asymptotically, that is, for large values of τ, the eigenvalue equation can be solved by means of $\mathbf{c}_1\sim e^{\pm i\omega\tau}$ yielding the dispersion relations from which we find the lower bound of the continuum spectrum. Thus we get

$$\lambda=i[\pm\omega(\delta-v)\pm(\tfrac{1}{2}\omega^2+q-\beta)], \tag{6}$$

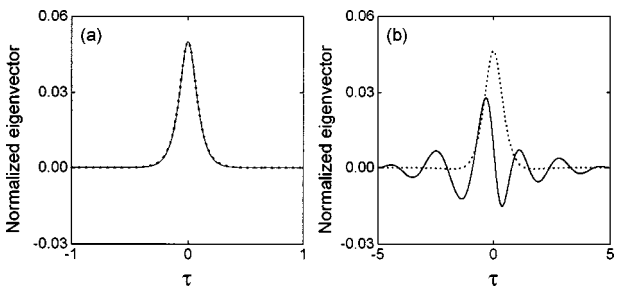

FIG. 7. (a) Internal normalized eigenvector corresponding to branch 8 in Fig. 6(b) at the point $v=1.2$, slightly before the critical point $v_c=1.215\,74$. (b) Internal normalized eigenvector corresponding to the point $v=2.162\,79$ slightly after the bifurcation point $v_c=2.160\,56$ where the branches 3 and 4 in Fig. 6(b) meet. Dots mark the neutrally stable eigenmode.

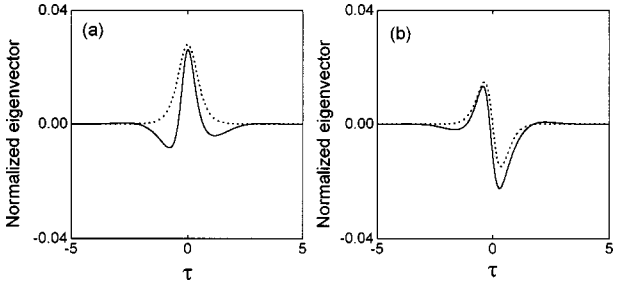

FIG. 8. Internal normalized eigenvector corresponding to the point $v=0.504$ slightly after the bifurcation point $v_c=0.505$ where the branches 1 and 2 in Fig. 6(a) fuse. In (a) U component, and in (b) V component. Dotted lines: the neutrally stable eigenvector (only the real part is shown).

and

$$\lambda=i[\pm\omega(\delta+v)\pm(\tfrac{1}{2}\omega^2+q+\beta)]. \tag{7}$$

The limit of the continuum spectrum is then given by

$$\lambda_c=i\,\min[q-\beta-(\delta-v)^2/2,\quad q+\beta-(\delta+v)^2/2] \tag{8}$$

for the vector solitons and

$$\lambda_c=i[q\pm\beta-(\delta\pm v)^2/2] \tag{9}$$

for the fast and slow solitons, respectively. Thus the eigenvalues of the continuous spectrum lie on the imaginary axis, namely on the rays $(\lambda_c,i\infty)$ and $(-\lambda_c,-i\infty)$.

The stationary solution of the dynamical system (1) are spectrally stable when the spectrum of the linearized operator $\mathbf{L}$ has no strictly positive real part. The linear eigenvalue problem has two localized states with the eigenvalue $\lambda=0$, corresponding to translational and phase invariance of Eq. (1). The other eigenvalues of the operator $\mathbf{L}$ arise in pairs $(\lambda,-\lambda)$ and $(\lambda^*,-\lambda^*)$ because the trace of the operator $\mathbf{L}$ is zero.

Figures 1–3 show the four kinds of existing families of stationary solitons. Figures 1(a)–3(a) show the families of stationary solutions presented in a Q-H diagram, for three representative values of the momentum $M=-6$, $M=1$, and $M=6$, whereas in Figs. 1(b)–3(b) we plot the dependence of the soliton energy on the soliton velocity for the same momentum values. Here the stable solitons are displayed with solid lines and the unstable ones with dashed lines. There exists a one-to-one correspondence between the points A and B in Figs. 1(a) and 1(b), between A and F in Figs. 2(a) and 2(b), and between the points A and D in Figs. 3(a) and 3(b). In agreement with the expectations, one finds that for a fixed momentum and for a given energy flow, the solitons realizing the absolute minimum of the Hamiltonian are dynamically stable [the lower full lines in Figs. 1(a)–3(a)]. Importantly, the lower full line in Fig. 1(a) corresponds to stable slow solitons for the chosen negative value of the momentum. The lower full line displayed in Fig. 2(a) corresponds to stable slow solitons until the crossing point F with the curve for in-phase solitons, then to stable in-phase solitons until the crossing point C with the curve for fast solitons, and finally

to the fast solitons beyond the point *C*. The lower full line in Fig. 3(a) is composed of two stable pieces: one piece corresponding to vector in-phase solitons until the crossing point *A* with the curve for fast solitons, and the other one corresponding to fast solitons beyond the point *A*. The sheets on the surface $H=H(Q,M)$ that correspond to higher values of *H* need special consideration. We have found that there exist also stable (or, more precisely, *metastable*) stationary solutions on these upper sheets, where the Hamiltonian has a local minimum. As shown in Figs. 1(a)–3(a), we have found that metastable vector out-of-phase solitons located in such an upper sheet also exist: the curves joining the points *A* and *B* in Figs. 1(a) and 2(a) [see also the inset in Fig. 1(a)] and the curves joining the points *B* and *C* in Fig. 3(a). There is an additional metastable branch of the fast mode connecting the points *C* and *D* in Figs. 2(a) and 2(b). Notice that for $M=1$ there exist two branches of the out-of-phase mode in different regions of the parameter space, namely, one branch joining the points *C* and *E* in Figs. 2(a) and 2(b), very close to the in-phase branch [see the inset in Fig. 2(a)], and the other one bifurcating from the fast mode at the point *A*. The small full line beyond the point *D* in Fig. 3(b) corresponds to the stable branch of the slow mode arising for rather large values of the energy and is not shown in Fig. 3(a).

Now we discuss the parametric dependence of the relevant Lyapunov eigenvalues in order to identify the bifurcations to complex-valued eigenvalues. The previously known instability scenario for the ground states (nodeless solutions) is related to the existence for $J>0$ of a pair of purely imaginary eigenvalues (with opoposite signs because of the Hamiltonian nature of the dynamical problem) lying in the gap [that is, ouside the interval $(-\lambda_c,\lambda_c)$]. These eigenvalues pass through zero at the bifurcation point where $J=0$ and then appear again as two purely real eigenvalues with opposite signs. At the point where the Jacobian *J* vanishes, the corresponding eigenvectors coincide with the neutrally stable modes (5) (see, e.g., [30]).

The outcomes of the Lyapunov eigenvalue calculations for $M=-6$, $M=1$, and $M=6$ are summarized in Figs. 4, 5, and 6, respectively, which show the values of the eigenvalues with the largest real part. As shown in the plot, we found that the soliton solutions destabilize either via the arising of *purely real eigenvalues* or via the arising of *complex eigenvalues* with nonzero real and imaginary parts.

We have evidentiated two instability scenarios, irrespective of the chosen values of the momentum (large negative, small positive, and large positive): (i) the standard instability described above related to the fact that the relevant eigenmode has a purely imaginary eigenvalue that passes through zero at the critical point and then becomes purely real, and (ii) the onset of instability is given by the appearance of a pair of complex-conjugate eigenvalues at the bifurcation point. This instability scenario is similar to that present in other physical settings, for example in the case of higher-order (TE_1) modes of nonlinear planar waveguides [18] and in the case of higher-order parametric solitons in quadratically nonlinear media which have a central peak and one or more surrounding rings (referred to as peak-and-ring solitons) [19].

We have found that the in-phase vector solitons are always stable [see Fig. 5(e)]. For the other modes, the general feature is that there are regions of instability separated by small regions of stability (or metastability) [see, for example, the regions marked by the curves 3, 4, and 5 in Figs. 4(b), 5(c), 5(d), and 6(b)]. In addition to the standard instability, which can be captured by asymptotic expansion around the neutrally stable eigenmode, we have identified the following bifurcation scenario: one internal eigenmode [line 4 in Fig. 4(a)] fuses with another internal eigenmode [line 3 in Fig. 4(a)], which emerges from the continuum spectrum. They form two pairs of eigenfunctions having complex-conjugate eigenvalues, giving the onset of the oscillatory instability. The same kind of instability is shown in Figs. 5(a), 5(c), and 5(d) (the lines 3 and 4), in Figs. 6(a) (the lines 1 and 2), and in Fig. 6(b) (the lines 3 and 4). The standard bifurcation scenario is illustrated in Figs. 4(b), 5(c), 5(d), 6(b), and 6(c).

In order to compare the two kinds of bifurcation, we have plotted in Figs. 7 and 8 the corresponding eigenvector profiles. In the case of standard bifurcation, the instability can be well described by asymptotic expansion around the neutrally stable eigenmode [see Fig. 7(a), where the internal eigenfunction profile is found to be very close to the zero mode profile], whereas for the other kind of bifurcation the eigenvector profiles are quite different from the neutrally stable eigenmodes [see Figs. 7(b), 8(a), and 8(b)]. These eigenvectors can be spatially extended, displaying rapid oscillations [see Fig. 7(b)].

III. CONCLUSIONS

We have shown that all slow, fast, walking vector in-phase, and vector out-of-phase solitons can be dynamically stable for appropriate values of the soliton parameters. Regarding the evolution of unstable solutions, the complex nature of the corresponding Lyapunov eigenvalues in some intervals of soliton parameters leads to a rich dynamical behavior, showing oscillatory exponential growth of small perturbations similar to those found for the fundamental modes of the generalized Thirring models [20].

The important result of this paper is the clear identification of the fact that the collision of two internal soliton modes gives the mechanism for the onset of oscillatory instabilities in the generalized Manakov model.

In conclusion, the cascade of bifurcations of lowest-order walking vector solitons of a generalized Manakov system discovered in this work, similar to those previously found for higher-order nonlinear modes in cubic [18] and quadratic [19] media, indicates that such instability scenarios may also exist for lowest-order states of other physical models. Thus, the complicated instability pattern presented in this paper may have important consequences for dynamical stability of multiparameter solitons in other Hamiltonian systems. We envisage that such results may be of interest both from a fundamental point of view in understanding nonlinear dynamics of conservative, Hamiltonian systems, and from an applicative point of view as well, whenever robustness of solitary waves is required.

ACKNOWLEDGMENTS

Useful correspondence and discussions with W. J. Firth and L. Torner are gratefully acknowledged.

[1] M.J. Ablowitz and P.A. Clarkson, *Solitons, Nonlinear Evolution Equations and Inverse Scattering* (Cambridge University Press, Cambridge, 1991).
[2] N.N. Akhmediev and A. Ankiewicz, *Solitons* (Chapman and Hall, London, 1997).
[3] G.P. Agrawal, *Nonlinear Fiber Optics* (Academic Press, San Diego, 1995).
[4] A. Hasegawa and Y. Kodama, *Solitons in Optical Communications* (Clarendon, Oxford, 1995).
[5] M.G. Vakhitov and A.A. Kolokolov, Izv. Vyssh. Uchebn. Zaved. Radiofiz. **16**, 1020 (1973) [Sov. Radiophys. **16**, 783 (1973)].
[6] E.A. Kuznetsov, A.M. Rubenchik, and V.E. Zakharov, Phys. Rep. **142**, 103 (1986).
[7] F.V. Kusmartsev, Phys. Rep. **183**, 1 (1989).
[8] K.J. Blow, N.J. Doran, and D. Wood, Opt. Lett. **12**, 202 (1987); E.M. Wright, G.I. Stegeman, and S. Wabnitz, Phys. Rev. A **40**, 4455 (1989); V.K. Mesentsev and S.K. Turitsyn, Opt. Lett. **17**, 1497 (1992); Y. Chen and J. Atai, Phys. Rev. E **52**, 3102 (1995); D.C. Hutchings and J.M. Arnold, J. Opt. Soc. Am. B **16**, 513 (1999).
[9] A.V. Buryak, Y.S. Kivshar, and S. Trillo, Phys. Rev. Lett. **77**, 5210 (1996); A.V. Buryak and Y.S. Kivshar, *ibid.* **78**, 3286 (1997).
[10] L. Torner, D. Mazilu, and D. Mihalache, Phys. Rev. Lett. **77**, 2455 (1996); D. Mihalache, D. Mazilu, L.-C. Crasovan, and L. Torner, Phys. Rev. E **56**, R6294 (1997); C. Etrich, U. Peschel, F. Lederer, and B. Malomed, *ibid.* **55**, 6155 (1997).
[11] J.M. Soto-Crespo, N. Akhmediev, and A. Ankiewicz, Phys. Rev. E **51**, 3547 (1995).
[12] N.J. Rodriguez-Fernandez and J.M. Soto-Crespo, J. Mod. Opt. **45**, 2039 (1998).
[13] L. Torner, D. Mihalache, D. Mazilu, and N.N. Akhmediev, Opt. Commun. **138**, 105 (1997).
[14] W. Chen and D.L. Mills, Phys. Rev. Lett. **58**, 160 (1987); A.B. Aceves and S. Wabnitz, Phys. Lett. A **141**, 37 (1989); D.N. Christodoulides and R.I. Joseph, Phys. Rev. Lett. **62**, 1746 (1989); C. M. De Sterke and J.E. Sipe, in *Progress in Optics XXXIII*, edited by E. Wolf (Elsevier, Amsterdam, 1994), pp. 203–260.
[15] B.J. Eggleton, R.E. Slusher, C.M. de Sterke, P.A. Krug, and J.E. Sipe, Phys. Rev. Lett. **76**, 1627 (1997).
[16] C. Conti, S. Trillo, and G. Assanto, Phys. Rev. Lett. **78**, 2341 (1997); H. He and P. Drummond, *ibid.* **78**, 4311 (1997); T. Peschel, U. Peschel, F. Lederer, and B.A. Malomed, Phys. Rev. E **55**, 4730 (1997).
[17] A.R. Champneys, B.A. Malomed, and M.J. Friedman, Phys. Rev. Lett. **80**, 4169 (1998).
[18] H.T. Tran, J.D. Mitchell, N.N. Akhmediev, and A. Ankiewicz, Opt. Commun. **93**, 227 (1992); N.N. Akhmediev, A. Ankiewicz, and H.T. Tran, J. Opt. Soc. Am. B **10**, 230 (1993).
[19] D.V. Skryabin and W.J. Firth, Phys. Rev. E **58**, R1252 (1998).
[20] A. De Rossi, C. Conti, and S. Trillo, Phys. Rev. Lett. **81**, 85 (1998); I.V. Barashenkov, D.E. Pelinovsky, and E.V. Zemlyanaya, *ibid.* **80**, 5117 (1998); J. Schöllmann, R. Scheibenzuber, A.S. Kovalev, A.P. Mayer, and A.A. Maradudin, Phys. Rev. E **59**, 4618 (1999).
[21] D. Mihalache, D. Mazilu, and L. Torner, Phys. Rev. Lett. **81**, 4353 (1998).
[22] S.V. Manakov, Zh. Éksp. Teor. Fiz. **65**, 505 (1973) [Sov. Phys. JETP **38**, 248 (1974)]; D.J. Kaup and B.A. Malomed, Phys. Rev. A **48**, 599 (1993).
[23] D.N. Christodoulides and R.I. Joseph, Opt. Lett. **13**, 53 (1988); M.V. Tratnik and J.E. Sipe, Phys. Rev. A **38**, 2011 (1988).
[24] N.N. Akhmediev, A.V. Buryak, and J.M. Soto-Crespo, Opt. Commun. **112**, 278 (1994); N.N. Akhmediev, A.V. Buryak, J.M. Soto-Crespo, and D.R. Andersen, J. Opt. Soc. Am. B **12**, 434 (1995).
[25] Yu.S. Kivshar and S.K. Turitsyn, Opt. Lett. **18**, 337 (1993); M. Haelterman, A.P. Sheppard, and A.W. Snyder, *ibid.* **18**, 1406 (1993); Y. Silberberg and Y. Barad, *ibid.* **20**, 246 (1995); C. Paré, Phys. Rev. E **54**, 846 (1996).
[26] C.R. Menyuk, IEEE J. Quantum Electron. **QE-23**, 174 (1987); **QE-25**, 2674 (1989); S.G. Evangelides, L.F. Mollenauer, J.P. Gordon, and N.S. Bergano, J. Lightwave Technol. **10**, 28 (1992).
[27] S. Trillo, S. Wabnitz, E.M. Wright, and G.I. Stegeman, Opt. Commun. **70**, 166 (1989); S. Wabnitz, S. Trillo, E.M. Wright, and G.I. Stegeman, J. Opt. Soc. Am. B **8**, 602 (1991); A.B. Aceves and S. Wabnitz, Opt. Lett. **17**, 25 (1992).
[28] M.N. Islam, *Ultrafast Fiber Switching Devices and Systems* (Cambridge U. Press, Cambridge, 1992).
[29] Y. Barad and Y. Silberberg, Phys. Rev. Lett. **78**, 3290 (1997).
[30] C. Etrich, U. Peschel, F. Lederer, B.A. Malomed, and Y.S. Kivshar, Phys. Rev. E **54**, 4321 (1996).